九州大学学術情報リポジトリ
Kyushu University Institutional Repository

Finite Element Analyses for Time-dependent and Depth-dependent Deformation of Articular Cartilage and Chondrocytes Under Constant Compression

Ihara, Maki
Department of Intelligent Machinery and Systems : Graduate Student

Murakami, Teruo
Department of Intelligent Machinery and Systems : Professor

Sawae, Yoshinori
Department of Intelligent Machinery and Systems : Associate Professor

https://hdl.handle.net/2324/1119

出版情報：九州大学工学紀要. 62 (4), pp.165-177, 2002-12-20. 九州大学大学院工学研究院
バージョン：
権利関係：

Memoirs of the Faculty of Engineering, Kyushu University, Vol. 62, No. 4, December 2002

Finite Element Analyses for Time-dependent and Depth-dependent Deformation of Articular Cartilage and Chondrocytes Under Constant Compression

by

Maki IHARA*, Teruo MURAKAMI** and Yoshinori SAWAE***

(Received September 24, 2002)

Abstract

Human joints are capable of functioning effectively with low friction and without failure throughout human life under circumstances where both articular cartilage as bearing material and synovial fluids as lubricants fulfill their normal functions. It is well accepted that articular cartilage adapts to changing mechanical environments. As the rubbring condition is getting severe, the articular cartilage will be worn, resulting in osteoarthritis, but little is known about the mechanism to osteoarthritis. It is important to clear the stress-strain state of cartilage and in chondrocytes under repeated cartilage deformation to know how osteoarthritis gets to start and progress. The purpose of this study is to investigate an influence of chondrocytes on stress-strain state of articular cartilage and an influence of position of chondrocytes on its depth-dependent deformation. FEM analyses predict that the time-dependent and depth-dependent deformation of articular cartilage is caused by fluid exudation, but material properties of chondrocytes do not affect the bulk deformation of articular cartilage so much. The deformation of chondrocytes is depth-dependent and the largest time-dependent deformation behavior occurs in the surface layer. These results may clear how the transduction of mechanical stimuli concern about metabolism of articular cartilage via chondrocytes.

Keywords: Biomechanics, Viscoelasticity, Finite Element Method, Articular Cartilage, Chondrocytes, Time-dependent deformation, Depth-dependent deformation, Stress-strain state

1. Introduction

It is well known that natural synovial joints would maintain the very low friction and low

*Graduate Student, Department of Intelligent Machinery and Systems
**Professor, Department of Intelligent Machinery and Systems
***Associate Professor, Department of Intelligent Machinery and Systems

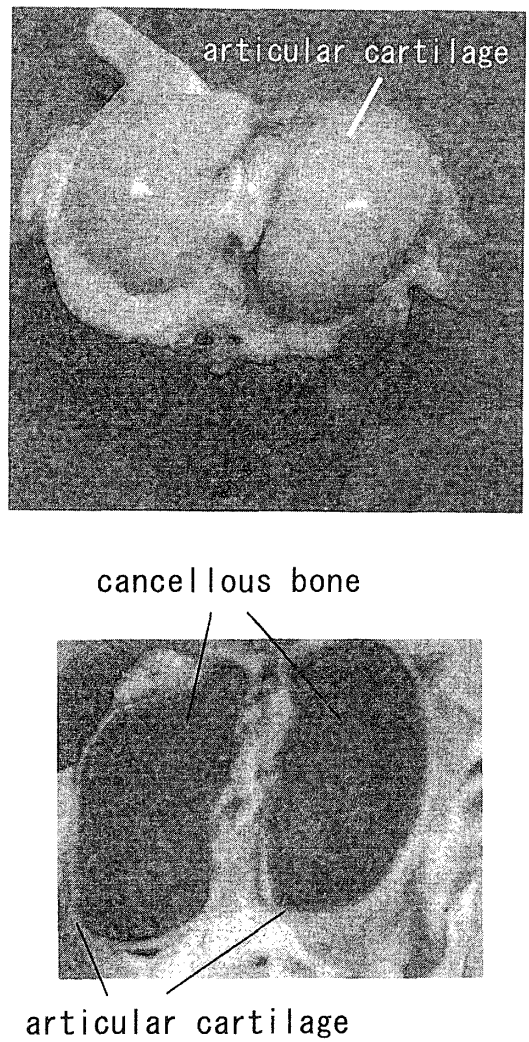

Fig. 1 Images of articular cartilage of porcine femoral condyle

wear throughout human life if the articular cartilage(**Fig. 1**) keeps up lubricated with healthy synovial fluids. It is considered that articular cartilage in natural synovial joints adapts to the changing of mechanical environments, where the chondrocytes can respond to local stress-strain state. Articular cartilage consists of chondrocyte (the cell in the articular cartilage) and extracellular matrix which is produced by chondrocyte. Mechanical compression of articular cartilage has a significant effect on the metabolic activity of the chondrocytes. Osteoarthritis which is a disease in synovial joint leads to degeneration of articular cartilage and arthromeningitis. It is known that chondrocytes have the important role in the mechanism how osteoarthritis gets to start and develop and the mechanical environment of the chondrocytes is an important factor that has been shown to have a significant influence on the health and disease of the diarthrodial joint. Therefore, the knowing the stress-strain states of chondrocytes during physiological loading in joints becomes a first step to the biomechanical understanding of articular cartilage adaptation and degeneration.

Articular cartilage has viscoelastic property based on high water content up to 80% and the fluid-flow behavior by significant amounts of mobile fluid concerns the time-dependent deformation of articular cartilage under compression. The content and structure of collagen and proteoglycan in articular cartilage vary with depth from the articulating surface. In the surface zone, collagen fibrils are organized parallel to the articular surface. In the middle zone, the collagen fibrils appear to be randomly arranged. In the deep zone, the collagen

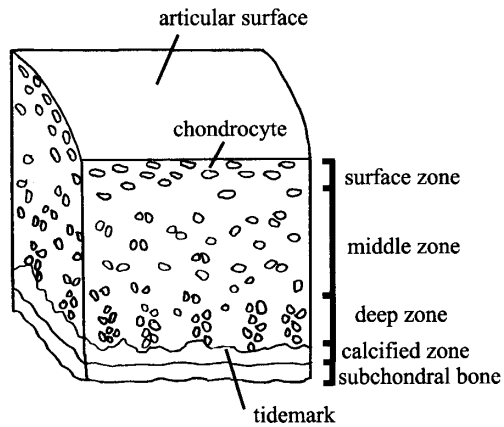

Fig. 2 Diagram of articular cartilage

fibers are organized perpendicular to the surface. The amount of proteoglycan is richer in the deep zone than in the surface zone. Chondrocytes are dispersed throughout the articular cartilage (**Fig. 2**) and make up about 10% of the tissue volume in adult cartilage. Chondrocytes are ellipsoid parallel to surface in the surface zone and are round grouping into pairs in the middle zone. In the deep zone, they are gathering up to about ten[1]. The elastic modulus of chondrocytes is smaller by three orders while the permeability of chondrocytes is greater by five orders than those of extracellular matrix[2)3)]. Because of the depth-dependent composition and huge difference in elastic moduli and permeabilities between chondrocytes and the surrounding extracellular matrix, the stress-strain fields in the cells are different from those of the surrounding matrix.

Assuming the articular cartilage as an elastic material (no fluid flow), the material properties of chondrocyte which is largely different from those of surrounding extracellular matrix do not affect the stress-strain state of articular cartilage. But in actual cartilage with high water content, it is predicted that the pattern of distribution of chondrocytes has a non-negligible effect on the stress-strain state of articular cartilage and chondrocytes because of fluid flow. Therefore it is important to elucidate the effect of material properties of chondrocytes on the time-dependent and depth-dependent stress-strain state of compressed articular cartilage when the tissue is exposed to compression.

The purpose of this study is to develop a simple model which can simulate the biomechanical behavior of articular cartilage. At first, we made the two models to research the influence of chondrocytes on stress-strain state of articular cartilage. We assumed that articular cartilage was categorized as three layers by composition and structure of articular cartilage to analyze the depth-dependent stress-strain state of articular cartilage. Second, we made the another model which has a chondrocyte in the tissue to clear the time-dependent and depth-dependent stress-strain state of chondrocytes under loading of articular cartilage.

2. Method

2.1 Constitutive equation

Articular cartilage was modeled using the biphasic theory[4)], which depicts hydrated tissues as a mixture of a porous, permeable elastic solid (proteoglycan, collagen, and chondrocytes) and a movable interstitial fluid.

$$\begin{aligned}&\boldsymbol{\sigma}^{s,i}=-\Phi^{s,i}p\mathbf{I}+\boldsymbol{\sigma}^{s}{}_{e}{}^{,i},\\&\boldsymbol{\sigma}^{s}{}_{e}{}^{,i},=\lambda_i\varepsilon_v\mathbf{I}+2\mu_i\boldsymbol{\varepsilon},\quad \boldsymbol{\sigma}^{f,i}=-\Phi^{f,i}p\mathbf{I},\\&\boldsymbol{\sigma}^{t,i}=\boldsymbol{\sigma}^{s,i}+\boldsymbol{\sigma}^{f,i}=-p\mathbf{I}+\boldsymbol{\sigma}^{s}{}_{e}{}^{,i},\ i=\mathrm{c,m},\end{aligned}\tag{1}$$

where $\mathbf{I}$ is the unit tensor; $\boldsymbol{\sigma}^s$, $\boldsymbol{\sigma}^f$, and $\boldsymbol{\sigma}^t$ represent the stresses in the solid phase, in the interstitial fluid, and in the total tissue; λ and μ are the first and second Lamé constants; p, $\boldsymbol{\varepsilon}$, and ε_v are fluid pressure, strain and volumetric strain of the solid phase; $\Phi^{s,i}$, and $\Phi^{f,i}$ $(\Phi^{s,i}+\Phi^{f,i}=1)$ are the solid and fluid volume fractions, respectively; superscripts c and m imply cell and matrix, respectively. λ and μ are connected with Young's modulus and Poisson's ratio as

$$E_i=\mu_i(3\lambda_i+2\mu_i)/(\lambda_i+\mu_i)\tag{2}$$

$$V_i=\lambda_i/2(\lambda_i+\mu_i)\tag{3}$$

The conservation of momentum is satisfied everywhere in cells and matrix

$$\begin{aligned}&\nabla\boldsymbol{\sigma}^{s,i}+(v^f-v^s)(\Phi^{f,i})^2/k_i=0,\\&\nabla\boldsymbol{\sigma}^{f,i}-(v^f-v^s)(\Phi^{f,i})^2/k_i=0\ ;\ i=\mathrm{c,m},\end{aligned}\tag{4}$$

where v^s and v^f are the velocities of solid and fluid, k_c and k_m are permeabilities of cells and matrix, respectively. The continuity condition holds everywhere in cells and matrix

$$\nabla(\Phi^{f,i}v^f+\Phi^{s,i}v^s)=0\ ;\quad i=\mathrm{c,m},\tag{5}$$

2.2 Compression test of macroscopic model

2.2.1 Mixture matrix

We used the two models of mixture matrix which consist of the material properties of chondrocytes and extracellular matrix to investigate the influence of material properties of chondrocyte (Young's modulus, Poisson's ratio and permeability) on the stress-strain state of articular cartilage. *Void model* is that chondrocytes within cartilage are supposed to be voids by dilute disperse (suspension) theory[6] for poro-elastic materials, in other words, the properties of chondrocytes were neglected, and *Cell model* is proposed by Wu et al[7]. Material properties of mixture matrix in each model were calculated by volume fraction of void and cell.

The mechanical properties of *Void model* are calculated as the following formula;

$$\mu=\mu_m\frac{(1-p_h)}{[1+6(K_m+2\mu_m)p_h/(9K_m+8\mu_m)]}\tag{6}$$

$$K=K_m\frac{(1-p_h)}{[1+3p_hK_m/4\mu_m]}\tag{7}$$

where μ and K are shear modulus and bulk modulus, respectively.

The mechanical properties and permeability k of *Cell model* are calculated as below,

$$\frac{d\mu}{d\Gamma}=\frac{(15K+20\mu)(\mu_c-\mu)\mu}{(6K+12\mu)\mu+(9K+8\mu)\mu}\tag{8}$$

$$\frac{dK}{d\Gamma}=\frac{(3K+4\mu)(K_c-K)}{(3K_c+4\mu)}\tag{9}$$

$$k=k_m\left[1+\frac{p_c}{(1-p_c)/3+[k_m/(k_c-k_m)]}\right] \tag{10}$$

p_h, p_c, are volume fraction of voids and chondrocytes and Γ is parameter of volume fraction $p_c=1-\exp(-\Gamma)$ ($p_c=0$: $\Gamma=0$; $p_c=1$: $\Gamma=\infty$) E and ν are calculated from μ and K.

$$E=9\mu K/(3K+\mu) \tag{11}$$

$$\nu=(3K-2\mu)/2(\mu+3K) \tag{12}$$

In addition, articular cartilage has a depth-dependent structure, which may cause the depth-dependent deformation of articular cartilage. Therefore, we supposed that articular cartilage are categorized as three layers and assumed that 10% zone from surface is surface layer, the medium 70% zone is middle layer and the deeper 20% zone is deep layer as shown in **Fig. 3**. Material properties of cell and extracellular matrix are shown in **Table 1**[8] and volume fraction of chondrocytes in each layer is shown in **Table 2**[1]. To estimate the volume fraction of chondrocytes, we took sequential fluorescent cross-sectional images of stained chondrocytes within articular cartilage by confocal laser scanning microscope (**Fig. 3**). Forty images were obtained at 1μm intervals. Categorizing articular cartilage as three layers just as explanation above, we calculated the volume fraction by integral calculus. Mixture material properties calculated from equation (11), (12) are shown in **Table 3**. The axisymmetric cylindrical specimen model in **Fig. 4** was assumed to have a thickness of 1mm and to

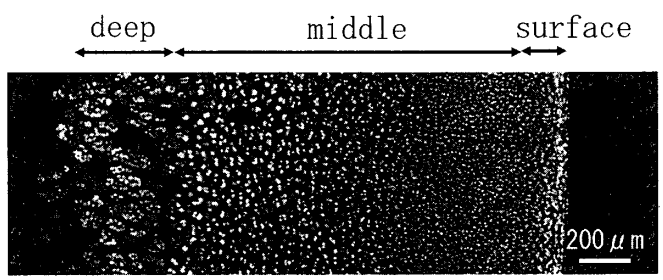

Fig. 3 Image of chondrocytes within articular cartilage of porcine

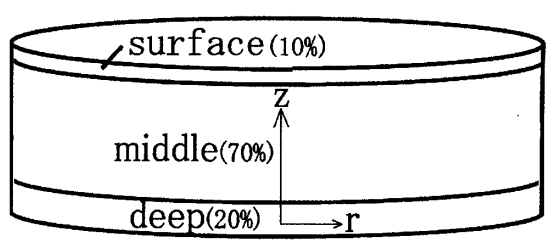

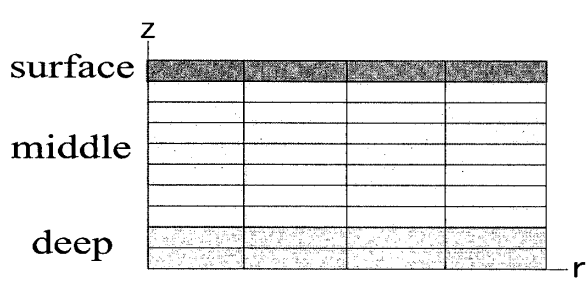

Fig. 4 Three layered FEM model

Table 1 Material properties of extracellular matrix and chondrocyte

Properties	E (MPa)	ν	k ($mm^4/N \cdot s$)
Extracellular matrix	1.0	0.125	2.0×10^{-3}
Chondrocyte	1.0×10^{-3}	0.2	2.0×10^{2}

Table 2 Volume fraction of each layer

Layer	surface	middle	deep
Volume fraction	7.3%	11.3%	7.3%

Table 3 Material properties of mixture material

	E(MPa)		ν		k ($\times 10^{-3}$ $mm^4/N \cdot s$)	
	void	cell	void	cell	void	cell
surface	0.865	0.859	0.130	0.131	2.0	2.47
middle	0.798	0.788	0.133	0.134	2.0	2.76
deep	0.865	0.859	0.130	0.131	2.0	2.47

have a diameter of 3mm. As finite element analysis, ABAQUS/Standard was applied[5]. For numerical analysis for biological soft tissues containing significant amounts of mobile tissue fluid, the mixture formulation based on biphasic theory and poroelastic theories are applied. It has been shown that the poroelastic and biphasic mixture models are equivalent when applied to biomechanical studies[5].

2.2.2 Boundary conditions

We simulated the unconfined compression test and the cartilage specimen was subjected to a ramp compression of $\varepsilon = 15\%$ strain of specimen thickness with a ramp period 1s (**Fig. 5**). The total strain was kept constant for 1200s. Undersurface of specimen was assumed to be firmly fixed with impermeable subchondral bone and the indentation plate was impermeable, where friction is neglected between the plate and articular cartilage. The lateral boundaries were assumed as permeable.

2.3 Compression test of the microscopic model

In this section, we analyzed the microscopic model including a cell in the center of specimen shown in **Fig. 6** to investigate the change of mechanical environment of chon-

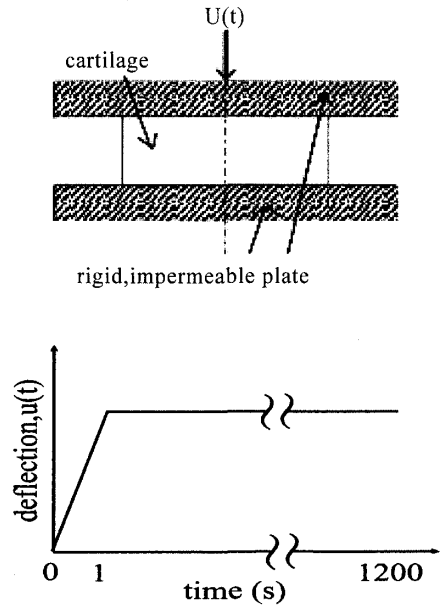

Fig. 5 Unconfined compression test

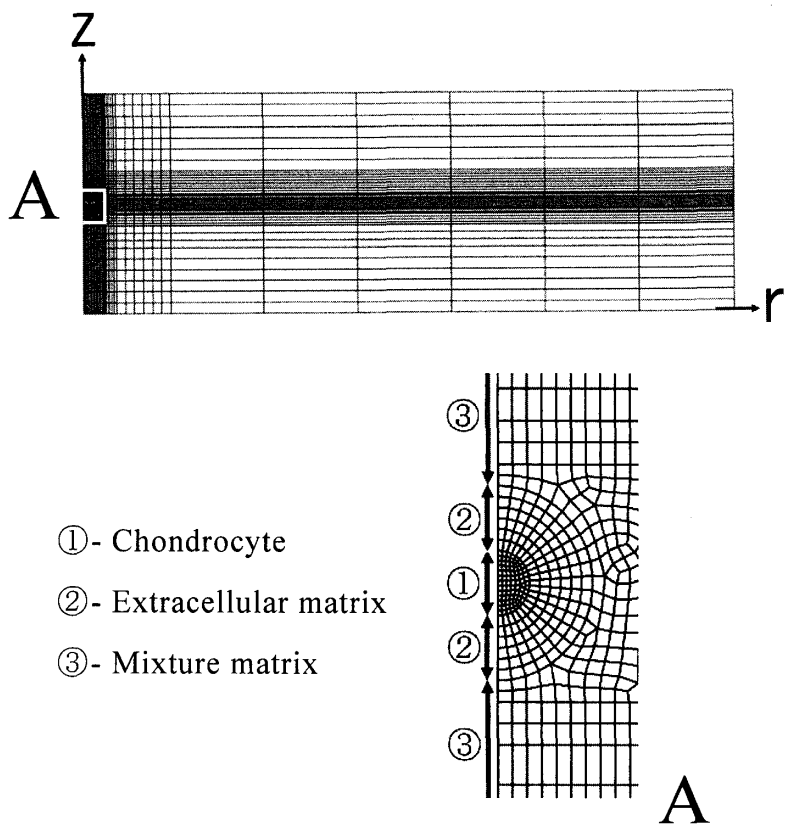

Fig. 6 Cartilage-model including a cell in the center

drocytes when the tissue is exposed to compression. We applied the *Cell model* to mixture matrix shown in **2.2.1**. To compare the analysis by Wu et al[7] with our analysis, the specimen is assumed to have a thickness of 1mm and to have a diameter of 6mm. Boundary conditions and material properties are the same way as section **2.2**. A diameter of cell is 20 μm and that

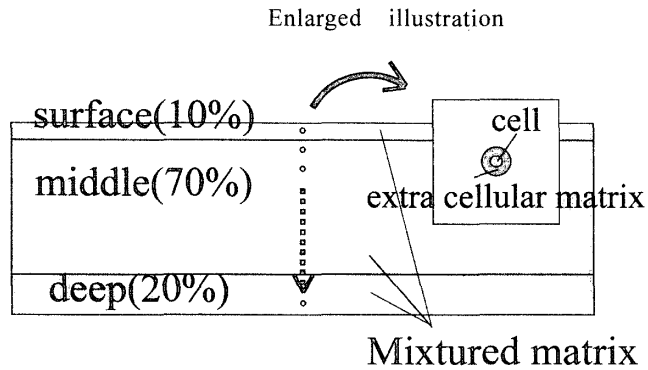

Fig. 7 Cartilage-model based on depth dependence of cell

of extracelullar matrix around the cell is 60 μm.

Furthermore, we made the depth-dependent model shown in **Fig. 7** to investigate how depth-dependent location of chondrocytes concern about the deformation of chondrocytes. We categorize articular cartilage as ten layers. In each analysis, we put a cell at the center in each layer.

3. Results

3.1 Compression test of macroscopic model

The equilibrium strains in three kinds of layer after 1200s are shown for both models in **Fig. 8**. The final values of strains have little difference between *Void model* and *Cell model*, because the volume fraction of chondrocytes in each layer is small and the final values of strain depend on the elastic modulus. But the time-dependent strain behavior for each model as shown in **Fig. 9** represent that time-dependent strains in the surface and deep layer show a little difference between *Void model* and *Cell model*. The strain of *Cell model* reached equilibrium faster than *Void model*. For example, the strain of the surface layer in *Cell model* is 112% of final strain and it is 115% of final strain in *Void model* at 130s after compression. This is caused by the difference in permeability because the permeability in *Cell model* is larger than *Void model*.

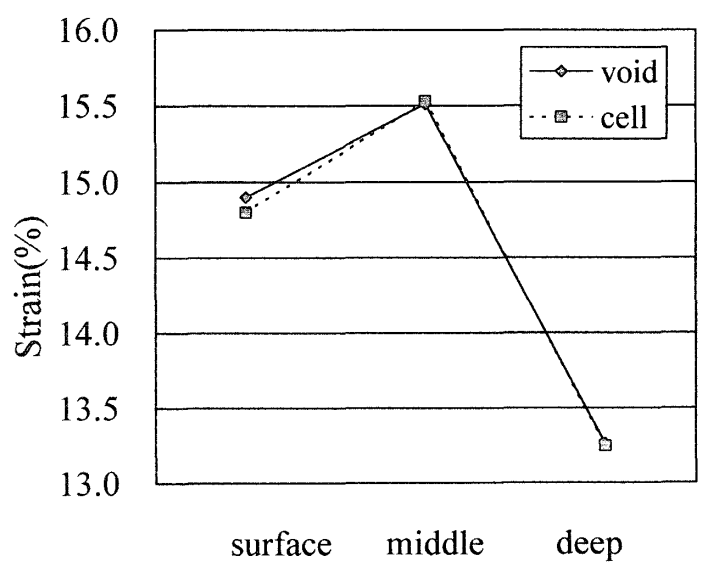

Fig. 8 Equilibrium strain of each layer (1200s passage after compression)

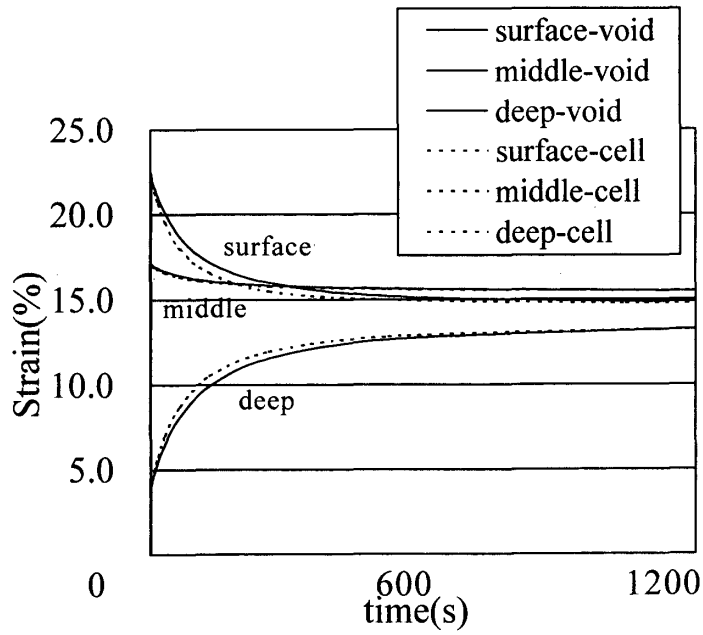

Fig. 9 Time-dependent strain of each layer

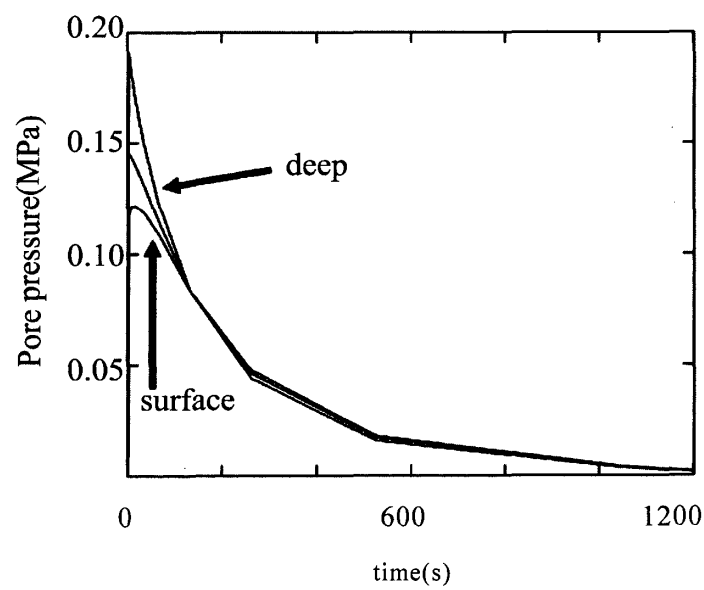

Fig.10 Time-dependent pore pressure of cell model
(each line shows the center value of each layer)

The larger strain than equilibrium strain was found in the surface in special because the compression propagated from the surface of specimen. With time, the strains of three layers gradually approaches to the equivalent values defined by the elastic modulus. This time-dependent behaviors are caused by the fluid flow in the biphasic articular cartilage, which correspond to the changes in pore pressure as shown in **Fig. 10**, where the pressure gradient induces the fluid flow. And this fluid flow produces the viscoelastic property of articular cartilage.

3.2 Compression test of microscopic model

The deformation of chondrocytes in the center of specimen is shown in **Fig. 11**. Immediately after compression, the height of the cell decreased by 31%, the width of the cell increased by 15%, and the volume of the cell decreased by 8%. At the end of the test ($t=$

1200s), the height of the cell decreased by 27%, the width of the cell increased by 2%, and the volume of the cell decreased by 23%.

The time-dependent changes in height, width and volume of chondrocytes which were located at varying depth are shown in **Figs.12, 13** and **14**. A cell in the first 10% layer is named as 1 and a cell in the second 10% layer is 2. Then the numerals from 3 to 10 correspond to cells in the third 10% layer to tenth 10% layers. For the change in height, the cells 1 to 6 had decreased largely just after compression and been recovering with time. The cells 7 to 10 had been decreasing with time. For the change in width, cells in all layers had increased immediately after compression, and been decreasing with time. A cell 1 changed largely in special. For the change in volume, a cell 1 had increased largely just after

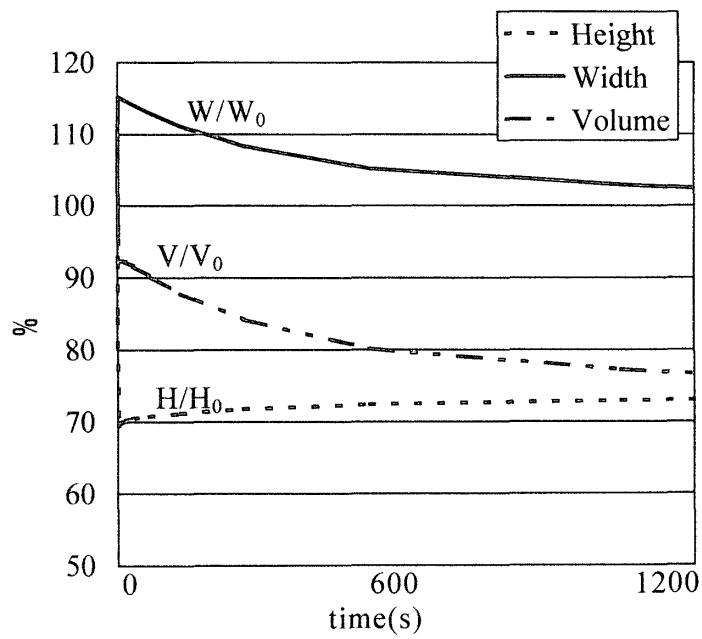

Fig.11 The height, width and volume of cell as a function of time for model shown in **Fig. 6**

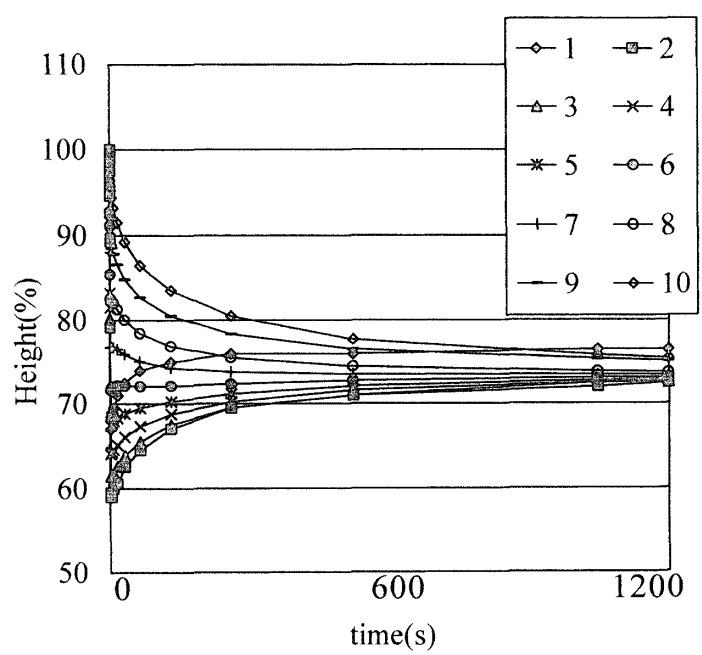

Fig.12 The height of cell as a function of time for model shown in **Fig. 7**

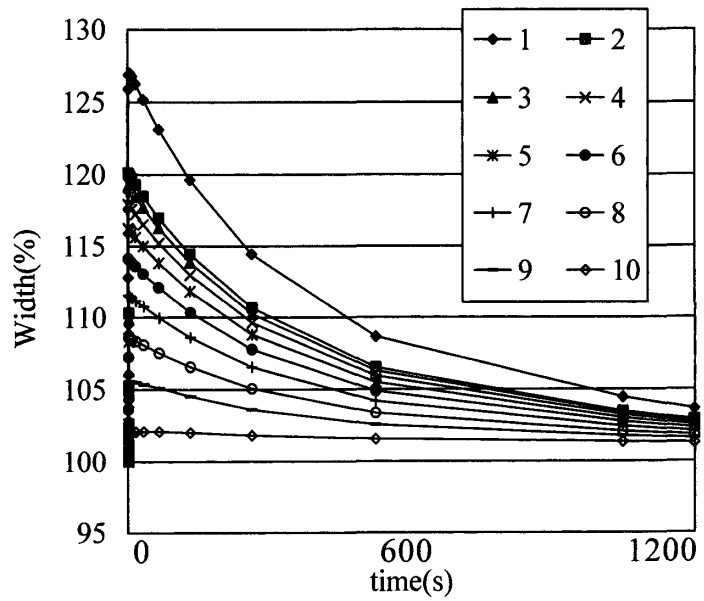

Fig.13 The width of cell as a function of time for model shown in **Fig. 7**

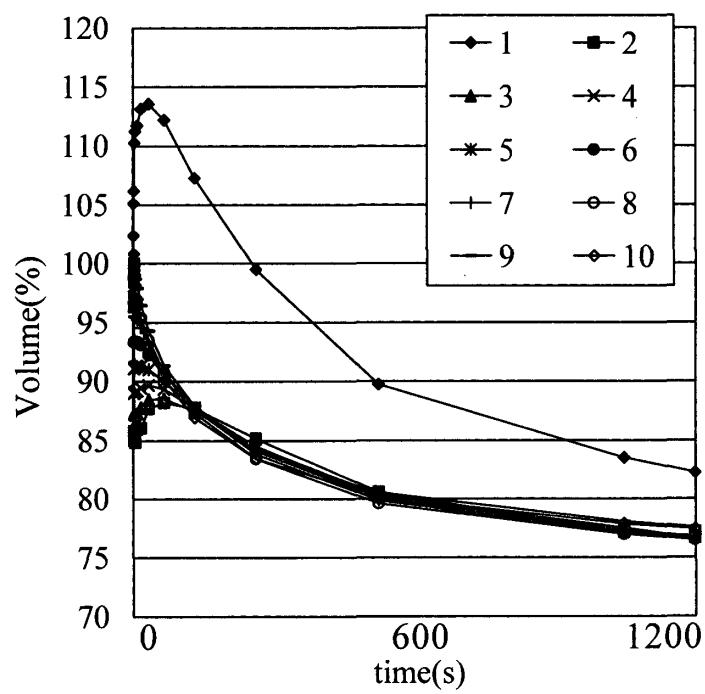

Fig.14 The volume of cell as a function of time for model shown in **Fig. 7**

compression and been decreasing with time. The cells 2 to 4 had decreased just after compression and been increasing, and then decreasing with time. The cells 5 to 10 had been gradually decreasing with time.

4. Discussions

We could study the time-dependent and depth-dependent stress-strain state of articular cartilage under compression in our FEM analyses. In our study, the dependence of the compressive deformation of cartilage on the material properties of chondrocytes could not be seen in compression test of macroscopic model, but a little difference was observed for the time-dependent strain of each layer. This time-dependency appears to be brought because the

high permeability of chondrocytes influences the fluid flow in the articular cartilage. It is known that material properties of chondrocyte would change depending on its condition[9]. But in the macroscopic level, the change in material properties of chondrocytes will be small and negligible.

The analysis on the cartilage deformation demonstrated that the strain levels of the surface and middle zones became larger than the average strain immediately after compression but finally reached the equilibrium strain determined by each elastic modulus. Compression from surface of the tissue causes this internal strain behavior. In actual cartilage, articular cartilage is fixed with subchondroal bone and is compressed from surface of tissue. Therefore, the similar stress-strain state would occur in actual cartilage as this FEM analysis.

At equilibrium state, our prediction on the strain of surface layer does not agree so well with the experimental observation by Guilak et al[10], who reported that the strain of surface layer would be the largest (19%), while highly strain of surface layer immediately after compression was shown but recovered to about 15% at equilibrium in our study. The difference between analysis and experiment may be brought because we used the same material properties of extracellular matrix in each three layer and furthermore, final strain of articular cartilage is determined by the elastic modulus. But in actual cartilage, articular cartilage has depth-dependent inhomogenity. The actual strain may be partly influenced by the inhomogenity of cartilage.

In our prediction of microscopic model, time-dependent shape change of chondrocyte could be evaluated. Cell height increased from 69% to 73% of the original cell height, cell width decreased from 115% to 102% of the original cell width, and the cell volume decreased from 92% to 77% of the original cell volume during a time period of 1200s when the deformation of cartilage was kept constant, which almost agree with the FEM analysis by Wu et al[7] who reported that the cell height increased from 67% to 70% of the original cell height, cell width decreased from 120% to 109% of the original cell width, and the cell volume decreased from 94% to 83% of the original cell volume under the same compression state. In addition, our prediction has the same behavior as the experimental observation by Guilak et al[10], who reported that chondrocytes in the middle to deep layers experience a decrease in height of 18.8-20.7%, a small expansion in width 1-4%, and a decrease in volume of 15.5-17.5 % in an unconfined compression test similar to that simulated here in FEM analysis.

The depth-dependent distribution of chondrocyte has influence on its shape change. In our prediction, cells in the surface and surface side of middle layer will be deformed largely just after compression of the tissue, and then they will recover with time and cells in the deep side of middle layer and deep layer will be compressed little by little. It is well accepted that the biological activity of chondrocytes play an important role for the metabolism of articular cartilage and it is influenced by the mechanical environment. It follows from our prediction that the chondrocytes in surface layer will contribute a significant viscoelastic component to the deformation behavior of the tissue[11] and will translate the gradual change of mechanical stimulus to chondrocytes in middle and deep layer.

5. Conclusions

We proposed the macroscopic and microscopic models for finite element analyses that can be used to demonstrate the time-dependent and depth-dependent deformation of articular cartilage and chondrocytes under physiological compression of the tissue. FEM analyses predict that the time-dependent and depth-dependent deformation of articular cartilage is

caused by fluid exudation, but material properties of chondrocytes do not affect the bulk deformation of articular cartilage so much. The deformation of chondrocytes is depth-dependent and the largest time-dependent deformation behavior occurs in the surface layer. These results may clear how the transduction of mechanical stimuli concern about metabolism of articular cartilage via chondrocytes.

References

1) M. Ihara, T. Murakami, Y. Sawae: Proc. of the JSME Annual Conf. (in Japanese), No. 01-1(2001), 175-176
2) Jones, W. R., et. al: Trans. of the Orthop. Res. Soc., 22(1), (1997), 199
3) Shin, D. and Athanasiou, K. A.: Trans. of the Orthop. Res. Soc., 22(1), (1997), 352
4) Mow, V. C., et. al: ASME J. of Bio. Eng. 102(1980), 73-84
5) Wu, J. Z., et. al: J. of Biomech., 31(1998), 165-169
6) R. Kondo: Takozairyo—Seishitsu to Riyou—(in Japanese), (1973), 165, Gihodo
7) Wu, J. Z., et. al: J. of Biomech., 32(1999), 563-572
8) Guilak, F., Mow, V. C.: J. of Biomech., 33(2000) 1663-1673
9) Trickey, W. R., et. al: J. Orthop. Res., 18(2000), 891-898
10) Guilak, F., et. al: J. Orthop. Res., 13(1995), 410-421
11) Guilak, F., et. al: Osteo. and Carti., 7(1999), 59-70